AIMS Mathematics, 9(10): 27930–27954.
DOI: 10.3934/math.20241356
Received: 19 July 2024
Revised: 07 September 2024
Accepted: 19 September 2024
Published: 27 September 2024

https://www.aimspress.com/journal/Math

Research article

Direction and stability of Hopf bifurcation in an eco-epidemic model with disease in prey and predator gestation delay using Crowley-Martin functional response

Sahabuddin Sarwardi[1], **Hasanur Mollah**[1], **Aeshah A. Raezah**[2] **and Fahad Al Basir**[3,*]

[1] Department of Mathematics and Statistics, Aliah University, IIA/27, New Town, Kolkata -700 160, India

[2] Department of Mathematics, Faculty of Science, King Khalid University, Abha 62529, Saudi Arabia

[3] Department of Mathematics, Asansol Girls' College, Asansol-4, West Bengal, India

* **Correspondence:** Email: fahadbasir@gmail.com.

Abstract: In this work, we have studied an eco-epidemic model using the Crowley-Martin functional response that includes disease in prey and gestation delay in the predator population. The model possesses three equilibria, namely the disease-free, Predator-free, and the interior equilibrium point. In addition, we examined the stability of the equilibrium points varying the infection rate and time delay parameter. Detailed analysis of Hopf bifurcation of the interior equilibrium point contains two situations: with delay and without delay. Moreover, we have studied the direction of the Hopf bifurcation and the stability of periodic solutions utilizing normal form theory and the center manifold theorem. It is emphasized that Hopf bifurcation occurs when the time delay exceeds the critical value and that the critical value of the delay is strongly impacted by the infection rate in prey. A detailed numerical simulation is provided to verify the analytical results.

Keywords: predator-prey model; Crowley-Martin functional response; gestation delay; stability and direction of Hopf-bifurcation; numerical simulations
Mathematics Subject Classification: 92D25, 92D30, 34C23, 34C25, 37G15

1. Introduction

Predator-prey interactions are among the most important interaction types in ecology and mathematical modeling because they are so prevalent in daily life [1]. These types of interaction models exhibit complicated dynamics and are highly elusive. Many diseases harm ecological groups,

and these infections often significantly affect population size [2]. Ecologists and mathematicians have taken an interest in these communities in recent years due to their mathematical analysis. This led to the development of numerous mathematical models illustrating disease in species, which are today essential resources for investigating the relationships between diverse populations, especially those involving prey and predator [3].

Since Lotka [4] and Volterra [5] first presented and assessed the basic predator-prey model, which is still being expanded upon every year, a great deal of work has been done. Anderson and May conducted the initial research on how epidemics affect predation [6]. A variation of the Lotka-Volterra prey-predator model that showed increased predation and no reproduction on infected prey was analyzed. These days, as disease spreads through population communication, it is imperative to examine the eco-epidemiological model from both an ecological and mathematical perspective. Many years have passed since the basic predator-prey model was first described and assessed by Lotka [4] and Volterra [5].

A true scenario in ecological species is the presence of disease in either the predator or prey populations or both, and it has been noted that infections by parasitic- or viral diseases are the primary cause of this kind of occurrence. While some studies examined diseases that only affected the prey population [7–11], others examined diseases that affected the predator population [12–15]. Still, others examined cases in which the infection affected both the prey and predator populations. One way to include the reciprocal interaction between predators is by altering the predators' operational reactions to predation. We add a functional reaction to the Crowley-Martin type response in our model, which offers a more realistic account of prey-predator interactions. A considerable amount of research on the Crowley-Martin functional response has been conducted recently [16–18]. Much research has been conducted on the Beddington-DeAngelis functional response, as well as the Holling type functional response [19–23].

Considering delays in time happen under almost all natural circumstances, time-delay models are significantly more realistic. It makes more sense to assume that the time required for the predator to complete the gestation period will cause its reproduction to be delayed rather than occurring immediately after its victim is consumed. By including temporal delays, these kinds of mathematical models display more intricate dynamics and adopt a more useful strategy for understanding the interactions between predator and prey. Consequently, throughout time, investigations have been conducted on more realistic models of interacting populations by introducing time delays into the biological models [24–27]. A large number of scholars established and analyzed delay induced predator-prey ecoepidemic models [12, 28–31]. In [12], a predator-prey model with infection in predator was studied with gestation delay. In [17], a mathematical model for a predator-prey type system with a Crowley-Martin functional response was presented and Hopf bifurcation of the coexisting equilibrium point has been analyzed. A time-delay predator-prey system with a Crowley-Martin functional response was developed and examined in [18].

Predator-prey models with infection in prey and gestation delay in predator were studied in [32, 33]. In [32], authors considered nonlinear infection rates and type-II functional responses for both infected and susceptible pray. In [33], Crowley-Martin type functional response function is assumed for both susceptible and infected pray. Here, we have assumed here Crowley-Martin type functional response for susceptible prey and a Beddington-DeAngelis (ratio-dependent) type functional response for infected prey. Moreover, in our predator-prey model, we assume a time delay in predator population due to its gestation period. In addition, we have provided the analysis for the occurrence, stability, and

direction of Hopf bifurcation of the interior equilibrium point of the proposed delay model.

The current study is structured using the following parts: We formulate the delay model using useful assumptions in the next section. Section 3 addresses the existence and viability of the equilibria as well as the positive invariance and boundedness of the solutions. Section 4 discusses the existence of Hopf bifurcation around the interior equilibrium point. The stability and direction of the Hopf bifurcation are discussed in Section 5. To demonstrate our theoretical findings, we provide a number of numerical simulations in Section 6. The conclusions are finally provided in Section 7.

2. The mathematical model

In this section, we derived the model consisting of three species: the vulnerable prey, the diseased prey, and the predator population. Now, to formulate the model, we make the following assumptions:

H1: We presume that infection only influence the prey populations. The whole prey population is split into two different groups when there is disease: the susceptible prey population, $x(t)$, and the infected population, $y(t)$, at any time (t), and $z(t)$ is the size of predator population at any time t.
H2: When infection and predation are absent, the population of vulnerable prey increases logistically at an inherent growth rate r and carrying capacity K. Since the infected prey populations are unable to procreate, it is hypothesized that they compete with the susceptible individuals for resources like food and space rather than developing immunity.
H3: A basic mass action β is used to determine the rate of infection. The illness only spreads within the prey population, and the vulnerable prey population contracts it through contact with the diseased prey.
H4: The disease-related deaths of the infected prey population eliminate the infected prey population, and let ν represent the infected prey population mortality rate.
H5: The predator population consumes the susceptible prey population with a Crowley-Martin functional response for the predation with maximum attack rate n. Here, a denotes the handling time, and b denotes magnitude of interference among predator.
H6: The predator population consumes the infected prey population with a ratio-dependent (Beddington-DeAngelis type) functional response for the predation with half capturing saturation constant c and maximum attack rate n [34, 35].
H7: Assume that h is the harvesting rate of the susceptible predator population, and e_1 and e_2 are the conversion efficiency of susceptible predator, and infected predator, respectively.
H8: We also assume that τ as the gestation time delay of the predator.

We have the following mathematical model based on the previously stated assumptions:

$$\begin{aligned}
\frac{dx}{dt} &= rx\left(1-\frac{x+y}{K}\right)-\frac{\beta xy}{\alpha+y}-\frac{mxz}{(a+x)(b+z)}\\
\frac{dy}{dt} &= \frac{\beta xy}{\alpha+y}-\frac{nyz}{cz+y}-\nu y,\\
\frac{dz}{dt} &= \frac{e_1 mx(t-\tau)z(t-\tau)}{(a+x(t-\tau))(b+z(t-\tau))}+\frac{e_2 ny(t-\tau)z(t-\tau)}{cz(t-\tau)+y(t-\tau)}-hz,
\end{aligned} \tag{1}$$

Let $\phi : [-\tau, 0] \to \mathbb{R}^3$ be equipped with the sup-norm,

$$\|\phi\| = \sup_{-\tau \le \gamma \le 0} \{|\phi_1(\gamma)|, |\phi_2(\gamma)|, |\phi_3(\gamma)|\},$$

where, $\phi = (\phi_1, \phi_2, \phi_3) \in C([-\tau, 0], \mathbb{R}^3)$. The Banach space of continuous functions is indicated by C. Since populations usually have non-negative values due to biological causes, the following are the assumed initial functions for the delay model (1):

$$\begin{aligned} & x(\gamma) = \phi_1(\gamma),\ y(\gamma) = \phi_2(\gamma),\ z(\gamma) = \phi_3(\gamma) \\ \text{with} \quad & \phi_i(\gamma) \ge 0,\ \gamma \in [-\tau, 0),\ \phi_i(0) > 0,\ i = 1, 2, 3. \end{aligned} \tag{2}$$

3. Basic properties of the model

The basic characteristics, including non-negativity and boundedness of the solutions, and the existence of equilibria of the delayed system (1), are demonstrated in this section.

3.1. Positive invariance

Lemma 1. *Under the given initial conditions in (2), all solutions of the delay model (1) are non-negative and bounded on* $[0, +\infty)$.

Proof. The first equation of (1) can be put in the following form:

$$\begin{aligned} & \frac{dx}{dt} - xg(x, y, z) = 0, \text{ where, } g(x, y, z) = r\left(1 - \frac{x + y}{K}\right) - \frac{\beta xy}{\alpha + y} - \frac{mz}{(a + x)(b + z)}, \\ & \Rightarrow \left[\frac{dx}{dt} - xg(x, y, z)\right] \exp\left(-\int_0^t g(x(\zeta), y(\zeta), z(\zeta))d\zeta\right) = 0, \\ & \Rightarrow \frac{d}{dt}\left[x \exp\left(-\int_0^t g(x(\zeta), y(\zeta), z(\zeta))d\zeta\right)\right] = 0, \\ & \Rightarrow x(t) = x(0) \exp\left(\int_0^t g(x(\zeta), y(\zeta), z(\zeta))d\zeta\right). \end{aligned}$$

Using initial conditions (2), $x(0) = \phi_1(0) > 0$, and thus $x(t) > 0$ for $t \ge 0$.

Thus the non-negativity of $x(t)$ is established. Now, using the method of steps [36, 37], we establish the non-negativity of the variables, $y(t)$ and $z(t)$.

From the second and the third equations of model (1), we can write

$$y'(t) \ge -\nu y(t) \text{ and } z'(t) \ge -hz(t). \tag{3}$$

This holds for all $t \in (0, T]$, where T is a positive constant. Applying the standard comparison principle on (3), we have $y(t) \ge 0$ and $z(t) \ge 0$, for all $t \in (0, T]$.

The non-negativity of y and z on the interval $t \in (T, 2T]$ is established by repeatedly applying the previous reasoning, and in the same way, for each subsequent interval $t \in (nT, (n + 1)T], n = 2, 3, \ldots$, to include all positive times.

Thus non-negativity of solutions of the system (1) is established. Now we show the boundedness of the solutions of the same system.

Let $w = e_1x(t-\tau) + e_2y(t-\tau) + z$. For any $\eta > 0$, we have

$$\frac{dw}{dt} + \eta w = re_1x(t-\tau)\left(1 - \frac{x(t-\tau)+y(t-\tau)}{K}\right) - \frac{(e_1-e_2)\beta x(t-\tau)y(t-\tau)}{\alpha + y(t-\tau)} - e_2\nu y(t-\tau),$$
$$- hz + \eta\left[e_1x(t-\tau) + e_2y(t-\tau) + z\right],$$
$$\leq e_1x(t-\tau)\left(r + \eta - \frac{x(t-\tau)}{K}\right) + e_2\left(\eta - \nu\right)y(t-\tau) + (\eta - h)z.$$

Choosing sufficiently small η such that $\eta < \nu\ \eta < h,\ \eta < \nu,$ and $\eta < \delta$ we get

$$\frac{dw}{dt} + \eta w \leq M\left(= \frac{K(\eta + r)e_1}{4}\right).$$

By use of Gronwall's inequality [38], we get

$$0 \leq w(t) \leq \frac{M}{\eta}\left(1 - e^{-\eta t}\right) + w_1(0)e^{-\eta t}.$$

Consequently, as $t \to \infty \implies 0 < w(t) < \frac{M}{\eta}$.

This suggests that any solution for the systems represented by (1) is bounded.

□

3.2. Existence of equilibria

There exist three equilibrium points in the prey-predator model (1) that have biological significance.

1. The predator-free equilibrium point $E_2(x_2, y_2, 0)$ with $x_2 = \frac{\nu(\alpha+y_2)}{\beta}$, where y_2 is the positive root of the cubic equation given by,

$$\psi(y) = l_0y^3 + l_1y^2 + l_1y + l_3 = 0, \tag{4}$$

where,

$$l_0 = r\left(\alpha\beta + \nu\right), l_1 = 2\alpha\left(\alpha\beta + \nu\right) + r\left(\alpha\nu - \beta\right), l_2 = r\alpha^2\left(\alpha\beta + \nu\right) + 2\alpha r\left(\nu\alpha - \beta\right) + \beta^2K,$$
$$l_3 = r\alpha^2\left(\nu\alpha - \beta\right).$$

If cubic (4) has at least one positive root, the predator free equilibrium point $E_2(x_2, y_2, 0)$ is feasible. The maximum number of positive roots of the cubic (4) in x_2 are listed in Table 1.

One can observe from equation (4) and Table 1 that for $\nu\alpha - \beta > 0$, Case-IV is applicable, which means there will be no root of (4). But, if $\nu\alpha - \beta < 0$, i.e. for $\beta > \nu\alpha$, any of the first three cases can occur, indicating that at least one positive root of (4) exists.
Using the above results, we establish the following proposition.

Proposition 1. *For $\beta > \nu\alpha$, the predator-free equilibrium E_2 is feasible.*

2. The disease-free equilibrium point $E_3(x_3, 0, y_3)$ with $x_3 = \frac{ah(b+z_3)z_3}{e_1m - h(b+z_3)z_3}$ and $z_3 = \sqrt{\frac{re_1x(K-x)}{hK}}$. Here, disease does not exist between the predator and the prey. It is possible to attain the equilibrium point E_3 if $x_3 < K$ and $h\left(b + z_3\right)z_3 < e_1m$.

Table 1. Different cases for the existence of multiple positive roots of (4).

Cases	sign of l_0	sign of l_1	sign of l_2	sign of l_3	no. of positive roots
I	+	−	+	−	3
II	+	+	−	−	1
III	+	−	−	−	1
IV	+	+	+	+	0

3. The interior equilibrium point $E^*(x^*, y^*, z^*)$ with

$$x^* = \left(\frac{\alpha + y^*}{\beta}\right)\left(\nu + \frac{nz^*}{cz^* + y^*}\right)$$
$$y^* = \left(\frac{cz^* + y^*}{e_2 n}\right)\left[h - \frac{e_1 m x^*}{(a + x^*)(b + z^*)}\right]$$
$$z^* = \frac{(b + z^*)(a + x^*)}{m}\left[r\left(1 - \frac{x^* + y^*}{K}\right) - \frac{iy^*}{\alpha + y^*}\right]$$

The equilibrium point E^* is feasible if it satisfies the conditions $h(a + x^*)(b + z^*) > e_1 m x^*$ and $r(K - x^* - y^*)(\alpha + y^*) > K\beta y^*$. When there is no specific formulation for the equilibrium points and more complexity in the system, doing the local stability analysis of the coexisting equilibrium point becomes difficult. However, a numerical integration of system (2) offers important information.

4. Local stability analysis and Hopf bifurcations

In this part, the local stability of each of the system's five potential equilibrium points, both with and without delay, is investigated. Additionally, we note how the parameter τ affects system (1). First, we compute the Jacobian matrix of system (1), which is provided by

$$J_E = \begin{bmatrix} c_{11} & c_{12} & c_{13} \\ c_{21} & c_{22} & c_{23} \\ d_{31}e^{-\lambda\tau} & d_{32}e^{-\lambda\tau} & c_{33} + d_{33}e^{-\lambda\tau} \end{bmatrix},$$

where

$$c_{11} = r\left(1 - \frac{2x + y}{K}\right) - \frac{\beta y}{\alpha + y} - \frac{maz}{(a + x)^2(b + z)},\ c_{12} = -\frac{x}{K} - \frac{\beta\alpha x}{(\alpha + y)^2},$$
$$c_{13} = -\frac{mbx}{(a + x)(b + z)^2},\ c_{21} = \frac{\beta y}{\alpha + y},\ c_{22} = \frac{\beta\alpha x}{(\alpha + y)^2} - \frac{ncz^2}{(cz + y)^2} - \nu,\ c_{23} = -\frac{ny^2}{(cz + y)^2},$$
$$d_{31} = \frac{e_1 maz}{(a + x)^2(b + z)},\ d_{32} = \frac{e_2 ncz^2}{(cz + y)^2},\ c_{33} = -h,\ d_{33} = \frac{e_1 mbx}{(a + x)(b + z)^2} + \frac{e_2 ny^2}{(cz + y)^2},$$

and the characteristic value is obtained by linearizing the delayed system.

Theorem 1. *If $A_1 < h,\ A_2 > 0$, and $A_3 > 0$, then the predator-free equilibrium point E_2 of system* (2) *is asymptotically stable in the absence of the time delay (i.e. when $\tau = 0$). For $h < A_1,\ A_2 > 0$, and $A_3 > 0$, E_2 experiences a Hopf bifurcation, where, A_1, A_2, and A_3 are given in the proof.*

Proof. The Jacobian matrix J_{E_2}, at E_2, has an eigenvalue $-h + A_1 e^{-\lambda_{2,1}\tau}$ and the remaining two eigenvalues satisfy

$$\lambda^2 + A_2\lambda + A_3 = 0, \tag{5}$$

$$\begin{aligned}
\text{where } A_1 &= e_2 n + \frac{e_1 m x_2}{b\,(a + x_2)},\\
A_2 &= -r\left(1 - \frac{2x_2 + y_2}{K}\right) + \frac{\beta y_2}{\alpha + y_2} - \frac{\beta\alpha x_2}{(\alpha + y)^2} - \nu,\\
A_3 &= r\left(1 - \frac{2x_2 + y_2}{K}\right)\left(\frac{\beta\alpha x_2}{(\alpha + y_2)^2} - \nu\right) - \frac{\beta\nu y_2}{\alpha + y_2} + \frac{\beta x_2 y_2}{K\,(\alpha + y_2)}.
\end{aligned}$$

Now, two cases may be raised.

Case I ($\tau = 0$):

For $\tau = 0$, the Jacobian matrix J_{E_2} has one eigenvalue $-h + A_1$ and the remaining eigenvalues are the roots of $\lambda^2 + A_2\lambda + A_3 = 0$. Thus, E_2 is stable if $A_1 < h,\ A_2 > 0$, and $A_3 > 0$.

Case II ($\tau > 0$):

We are now attempting to identify the critical values of τ at which the real components of the roots of the characteristic equation change from negative to positive.

Finding a purely imaginary root $i\omega_2,\ \omega_2 \in R$ is our first step. After splitting the real and imaginary components of $\lambda_{2,1} = i\omega_2$ in (5), we may eliminate τ. This gives us

$$\omega_2^2 = A_1^2 - h^2. \tag{6}$$

If $A_1 > h$, then $\omega_2 \in R$, and this suggests that adding a delay to the model may result in a Hopf bifurcation. □

Theorem 2. *The equilibrium E_3 of system* (1) *is asymptotically stable when there is no time delay for $\beta c x_3 < \alpha\,(n + \nu c)$, $B_1 + B_3 > 0$, and $B_2 + B_4 > 0$. It can undergo a Hopf-bifurcation when the time delay (τ) crosses a critical value if $\beta c x_3 < \alpha\,(n + \nu c)$ and $B_2^2 - B_4^2 < 0$, where B_1, B_2, B_3, and B_4 are shown below.*

Proof. At $E_3(x_3, 0, z_3)$, the eigenvalues of J_{E_3} are

$$\lambda_{3,1} = \frac{\beta x_3}{\alpha} - \frac{n}{c} - \nu, \tag{7}$$

and other the two eigenvalues $\lambda_{3,2}$ and $\lambda_{3,3}$ are the roots of the following equation

$$\lambda^2 + B_1\lambda + B_2 + (B_3\lambda + B_4)\,e^{-\lambda\tau} = 0, \tag{8}$$

$$\text{where } B_1 = h - r\left(1 - \frac{2x_3 + y_3}{K}\right) + \frac{maz_3}{(a + x_3)^2 (b + z_3)},$$
$$B_2 = -h\left[r\left(1 - \frac{2x_3 + y_3}{K}\right) - \frac{maz_3}{(a + x_3)^2 (b + z_3)}\right],$$
$$B_3 = -\frac{e_1 mbx_3}{(a + x_3)(b + z_3)^2}$$
$$B_4 == r\left(1 - \frac{2x_3 + y_3}{K}\right)\left[\frac{e_1 mbx_3}{(a + x_3)(b + z_3)^2}\right]$$

Case I ($\tau = 0$):

One eigenvalue of J_{E_3} is $\frac{\beta x_3}{\alpha} - \frac{n}{c} - \nu$, and the remaining two eigenvalues satisfy

$$\lambda^2 + (B_1 + B_3)\lambda + B_2 + B_4 = 0.$$

Thus, for $\tau = 0$, E_3 will be asymptotically stable if $B_1 + B_3 > 0, B_2 + B_4 > 0$ and $icx_3 < \alpha(n + \nu c)$, otherwise it is unstable.

Case II ($\tau > 0$):

We now study the Hopf bifurcation taking τ as the bifurcation parameter to find out how the time delay τ affects the stability. To get a purely imaginary root $i\omega_3$, $\omega_3 \in R$, we start by examining (7). Subtracting τ from it and breaking it down into its real and imaginary parts yields

$$\omega_3^4 + \left(B_1^2 - B_3^2 - 2B_2\right)\omega_3^2 + B_2^2 - B_4^2 = 0. \tag{9}$$

Let $p = \omega_3^2$. Then, (8) becomes

$$P(p) = p^2 + \left(B_1^2 - B_3^2 - 2B_2\right)p + B_2^2 - B_4^2 = 0 \tag{10}$$
$$B_1^2 - B_3^2 - 2B_2 = h^2 + \left[r\left(1 - \frac{2x_3 + y_3}{K}\right) + \frac{maz_3}{(a + x_3)^2 (b + z_3)}\right]^2 + \left(\frac{e_1 mbx_3}{(a + x_3)(b + z_3)^2}\right)^2$$

$$B_2^2 - B_4^2 = h^2\left[r\left(1 - \frac{2x_3 + y_3}{K}\right) - \frac{maz_3}{(a + x_3)^2 (b + z_3)}\right]^2 - \left[r\left(1 - \frac{2x_3 + y_3}{K}\right)\left(\frac{e_1 mbx_3}{(a + x_3)(b + z_3)^2}\right)\right]^2.$$

It can be noted that if $B_2^2 - B_4^2 < 0$, then $P(p)$ has a positive real root. Consequently, we can get a pair of purely imaginary roots. We will use MATLAB simulation to show how time delay results in a Hopf bifurcation. □

Here, our main aim is to investigate how, in the presence of prey, predator, and disease, time delay influences the dynamic behavior of system (1) at the interior equilibrium point $E^*(x^*, y^*, z^*)$.

The following characteristic equation of the system at $E^*(x^*, y^*, z^*)$ is given by

$$\lambda^3 + s_1\lambda^2 + s_2\lambda + s_3 + \left(s_4\lambda^2 + s_5\lambda + s_6\right)e^{-\lambda\tau} = 0, \tag{11}$$

where

$$s_1 = h + \nu - r\left(1 - \frac{2x^* + y^*}{K}\right) + \frac{iy^*}{\alpha + y^*} - \frac{maz^*}{(a + x^*)^2 (b + z^*)} - \frac{\beta\alpha x^*}{(\alpha + y^*)^2} + \frac{ncz^{*2}}{(cz^* + y^*)^2},$$

$$
\begin{aligned}
s_2 &= \left[r\left(1-\frac{2x^*+y^*}{K}\right)-\frac{\beta y^*}{\alpha+y^*}-\frac{maz^*}{(a+x^*)^2(b+z^*)}\right]\left[\frac{\beta\alpha x^*}{(\alpha+y^*)^2}-\frac{ncz^{*2}}{(cz^*+y^*)^2}-\nu-h\right]\\
&\quad -h\left[\frac{\beta\alpha x^*}{(\alpha+y^*)^2}-\frac{ncz^{*2}}{(cz^*+y^*)^2}-\nu\right]+\frac{\beta y^*}{\alpha+y^*}\left(\frac{x^*}{K}+\frac{\beta\alpha x^*}{(\alpha+y^*)^2}\right),\\
s_3 &= h\left[r\left(1-\frac{2x^*+y^*}{K}\right)-\frac{\beta y^*}{\alpha+y^*}-\frac{maz^*}{(a+x^*)^2(b+z^*)}\right]\left[\frac{\beta\alpha x^*}{(\alpha+y^*)^2}-\frac{ncz^{*2}}{(cz^*+y^*)^2}-\nu\right]\\
&\quad -h\frac{\beta y^*}{\alpha+y^*}\left(\frac{x^*}{K}+\frac{\beta\alpha x^*}{(\alpha+y^*)^2}\right)\\
s_4 &= -\frac{e_1mbx^*}{(a+x^*)(b+z^*)^2}+\frac{e_2ny^{*2}}{(cz^*+y^*)^2},\\
s_5 &= \left(\frac{e_1mbx^*}{(a+x^*)(b+z^*)^2}+\frac{e_2ny^{*2}}{(cz^*+y^*)^2}\right)\left[r\left(1-\frac{2x^*+y^*}{K}\right)-\frac{\beta y^*}{\alpha+y^*}-\frac{maz^*}{(a+x^*)^2(b+z^*)}\right]\\
&\quad +\left(\frac{e_1mbx^*}{(a+x^*)(b+z^*)^2}+\frac{e_2ny^{*2}}{(cz^*+y^*)^2}\right)\left(\frac{\beta\alpha x^*}{(\alpha+y^*)^2}-\frac{ncz^{*2}}{(cz^*+y^*)^2}-\nu\right)-\frac{e_1m^2abx^{*2}}{(a+x^*)^3(b+z^*)^3}\\
&\quad +\frac{e_2cn^2y^{*2}z^{*2}}{(cz^*+y^*)^4},\\
s_6 &= \left[\frac{he_2ncz^{*2}}{(cz^*+y^*)^2}+\left(\frac{e_1mbx^*}{(a+x^*)(b+z^*)^2}+\frac{e_2ny^{*2}}{(cz^*+y^*)^2}\right)\left(\frac{\beta\alpha x^*}{(\alpha+y^*)^2}-\frac{ncz^{*2}}{(cz^*+y^*)^2}-\nu\right)\right]\\
&\quad \times\left[-r\left(1-\frac{2x^*+y^*}{K}\right)+\frac{\beta y^*}{\alpha+y^*}+\frac{maz^*}{(a+x^*)^2(b+z^*)}\right]\\
&\quad -\left(\frac{\beta y^*}{\alpha+y^*}\right)\left(\frac{x^*}{K}-\frac{\beta\alpha x^*}{(\alpha+y^*)^2}\right)\left[\frac{e_1mbx^*}{(a+x^*)(b+z^*)^2}+\frac{e_2ny^{*2}}{(cz^*+y^*)^2}\right]\\
&\quad +\left(\frac{x^*}{K}-\frac{\beta\alpha x^*}{(\alpha+y^*)^2}\right)\left(\frac{e_1maz^*}{(a+x^*)^2(b+z^*)}\right)\left(\frac{ny^{*2}}{(cz^*+y^*)^2}\right)-\left(\frac{mbx^*}{(a+x^*)(b+z^*)^2}\right)\\
&\quad \times\left[\left(\frac{\beta y^*}{\alpha+y^*}\right)\left(\frac{e_2ncz^{*2}}{(cz^*+y^*)^2}\right)-\left(\frac{ny^{*2}}{(cz^*+y^*)^2}\right)\left(\frac{e_1mbx^*}{(a+x^*)(b+z^*)^2}+\frac{e_2ny^{*2}}{(cz^*+y^*)^2}\right)\right]
\end{aligned}
$$

Case I ($\tau = 0$):

When $\tau = 0$, that is, there is no time delay, the characteristic equation becomes

$$\lambda^3 + S_1\lambda^2 + S_2\lambda + S_3 = 0, \tag{12}$$

where,

$$S_1 = (s_1 + s_4),\ S_2 = s_3 + s_6 > 0,\ S_3 = (s_3 + s_6).$$

The Routh-Hurwitz criterion gives the conditions for the asymptotic stability of E^* as

$$S_1 > 0,\ S_2 > 0,\ S_1S_2 - S_3 > 0. \tag{13}$$

We now examine the local Hopf bifurcation taking the infection rate β as the main parameter. Consequently, the following theorem is derived for the occurrence of local Hopf bifurcation.

Theorem 3. *At the interior equilibrium E^*, system (1) experiences a Hopf bifurcation when $\beta = \beta^*$ is included in Γ_{HB}, where*

$$\Gamma_{HB} = \left\{\beta \in R^+ : \ S_1(\beta^*)S_2(\beta^*) - S_3(\beta^*) = 0, \ \textit{with } S_2 > 0, \ \dot{S_3} - (\dot{S_1}S_2 + S_1\dot{S_2}) \neq 0\right\} \tag{14}$$

Proof. For $S_1S_2 - S_3 = 0$, the characteristic equation (12) takes the following form:

$$(\rho^2 + S_2)(\rho + S_1) = 0. \tag{15}$$

The three roots of the above equation are $\rho_1 = +i\sqrt{S_2}$, $\rho_2 = -i\sqrt{S_2}$, and $\rho_3 = -S_1$. For $S_1S_2 - S_3 = 0$, we thus have two purely imaginary eigenvalues. Verification of the transversality condition is necessary to validate the Hopf bifurcation. To do this, we differentiate characteristic equation (12), with respect to the bifurcation parameter β:

$$\begin{aligned}\frac{d\rho}{d\beta} &= \frac{\rho^2\dot{S_1} + \rho\dot{S_2} + \dot{S_3}}{3\rho^2 + 2\rho S_1 + S_2}\Big|_{\rho = i\sqrt{S_2}} \\ &= \frac{\dot{S_3} - (\dot{S_1}S_2 + S_1\dot{S_2})}{2(S_1^2 + S_2)} + i\Big[\frac{\sqrt{S_2}(S_1\dot{S_3} + S_2\dot{S_2} - S_1\dot{S_1}S_2)}{2S_2(S_1^2 + S_2)}\Big].\end{aligned}$$

This gives the following result:

$$\frac{dRe\,\rho}{d\beta}\Big|_{\beta=\beta^*} = \frac{\dot{S_3} - (\dot{S_1}S_2 + S_1\dot{S_2})}{2(S_1^2 + S_2)} \neq 0 \Leftrightarrow \dot{S_3} - (\dot{S_1}S_2 + S_1\dot{S_2}) \neq 0. \tag{16}$$

Thus, the transversality condition is verified, and the occurrence of Hopf bifurcation at $\beta = \beta^*$ is ensured. □

Case II ($\tau > 0$):

We now investigate how time delay τ affects the stability of interior equilibrium. Actually, the aim here is to find a biologically meaningful periodic orbit. The existence of Hopf bifurcation is established using the following theorem.

Theorem 4. *Suppose that for system* (1)*, the coexisting equilibrium point $E^*(x^*, y^*, z^*)$ is locally asymptotically stable when $\tau \in [0, \tau_*)$ for for $\tau < \tau_*$, and unstable for for $\tau > \tau_*$. Hopf bifurcation occurs at $\tau = \tau_*$ when the transversality condition $P_1P_3 + P_2P_4 > 0$ is satisfied.*

Proof. To obtain the periodic solution of (1) (i.e. occurrence of Hopf bifurcation), we need a pair of purely imaginary roots of the characteristic equation (11).

Let us assume $\lambda = i\omega(\omega > 0)$ is a purely imaginary root of (11). The following equations can be obtained by equating the real and imaginary portions:

$$(s_6 - s_4\omega^2)\cos(\omega\tau) + s_5\omega\sin(\omega\tau) = s_1\omega^2 - s_3 \tag{17}$$

$$(s_6 - s_4\omega^2)\sin(\omega\tau) - s_5\omega\cos(\omega\tau) = s_2\omega - \omega^3 \tag{18}$$

which gives

$$\sin(\omega\tau) = \frac{\omega\left[s_4\omega^4 + (s_1s_5 - s_6 - s_4s_2)\,\omega^2 + s_6s_2 - s_5s_3\right]}{s_4^2\omega^4 + \left(s_5^2 - 2s_6s_4^2\right)\omega^2 + s_6^2}. \tag{19}$$

$$\cos(\sigma\tau) = \frac{(s_5 - s_1 s_4)\omega^4 + (s_1 s_6 - s_2 s_5 + s_4 s_3)\,\omega^2 - s_6 s_3}{s_4^2\omega^4 + \left(s_5^2 - 2s_6 s_4^2\right)\omega^2 + s_6^2}. \tag{20}$$

Squaring and then adding both sides of (19) and (20), we finally obtain

$$\begin{aligned} &\omega^6 + t_1\omega^4 + t_2\omega^2 + t_0 = 0, \\ &t_2 = s_1^2 - s_2 - s_4^2, \\ &t_1 = s_2^2 - 2s_1 s_3 - 2s_6 s_4, \\ &t_0 = s_3^2 - s_6^2 - s_5^2. \end{aligned} \tag{21}$$

Let ω_* be the root of the equation (21). After solving (19) and (20), we obtain

$$\tau_k = \frac{1}{\omega_*}\arctan\left[\frac{\omega_*\left[s_4\omega_*^4 + (s_1 s_5 - s_6 - s_4 s_2)\,\omega_*^2 + s_6 s_2 - s_5 s_3\right]}{(s_5 - s_1 s_4)\omega_*^4 + (s_1 s_6 - s_2 s_5 + s_4 s_3)\,\omega_*^2 - s_6 s_3}\right] + \frac{2k\pi}{\omega_*}, \quad k = 0, 1, 2, 3...$$

We will now investigate the transversality condition of the Hopf bifurcation. When (11) is differentiated with respect to τ, it yields

$$\left(\frac{d\lambda}{d\tau}\right)^{-1} = \frac{\left(3\lambda^2 + 2s_1\lambda + s_2\right)e^{\lambda\tau} + 2s_4\lambda + s_5}{\lambda\left(s_4\lambda^2 + s_5\lambda + s_6\right)} - \frac{\tau}{\lambda}.$$

Following easy but conventional computations, we obtain

$$\Re\left[\frac{d\lambda}{d\tau}\right]^{-1}_{\lambda=i\omega_*,\tau=\tau_*} = \frac{P_1 P_3 + P_2 P_4}{P_3^2 + P_4^2},$$

where $P_1 = \left(s_2 - 3\omega_*^2\right)\cos(\omega_*\tau_*) - 2s_1\omega_*\sin(\omega_*\tau_*) + s_5,$

$P_2 = \left(s_2 - 3\omega_*^2\right)\sin(\omega_*\tau_*) + 2s_1\omega_*\cos(\omega_*\tau_*) + 2s_4,$

$P_3 = -s_5\omega_*^2$

$P_4 = s_4\omega_*^3 - s_6\omega_*$

But the sign of $\left[\frac{d(\Re(\lambda))}{d\tau}\right]_{\lambda=i\omega_*,\tau=\tau_*}$ is same as the sign of $\Re\left[\frac{d\lambda}{d\tau}\right]_{\lambda=i\omega_*,\tau=\tau_*}$. Therefore, the transversality condition $\Re\left[\frac{d\lambda}{d\tau}\right]_{\lambda=i\omega_*,\tau=\tau_*} > 0$ holds as if $(H_3) : P_1P_3 + P_2P_4 > 0$, and consequently the occurrence of Hopf bifurcation is established. □

5. Direction and stability of Hopf bifurcation

The following theorem states the results.

Theorem 5. *For the model system (1), if $n_1 > 0$ ($n_1 < 0$), then the Hopf bifurcation is supercritical (sub-critical). If $n_2 < 0$ ($n_2 > 0$), then the bifurcating periodic solutions are stable (unstable). If $T_2 > 0$ ($T_2 < 0$), then the bifurcating periodic solutions are increasing (decreasing). The parameters are given below and derived in the proof:*

$$B_1(0) = \frac{i}{2\tau^*\sigma^*}\left(g_{11}g_{20} - 2|g_{11}|^2 - \frac{|g_{02}|^2}{3}\right) + \frac{g_{21}}{2},$$

$$n_1 = -\frac{\Re\{B_1(0)\}}{\Re\{\lambda'(\tau^*)\}},$$
$$n_2 = 2\Re(B_1(0)),$$
$$T_2 = -\frac{\Im\{B_1(0)\} + \eta_1 \Im(\lambda'(\tau^*))}{\tau^*\sigma^*}.$$

Proof. The center manifold theorem and normal form theory have been applied in accordance with Hassard's concept [39] to examine the direction of the Hopf bifurcation and stability of bifurcated periodic solutions.

Let $\tau = \tau^* + \mu, \mu \in R$. Then $\mu = 0$ is the Hopf bifurcation value of system (1). Re-scaling the time delay $t \to (\frac{t}{\tau})$, then system (1) is then re-written as

$$\dot{w}(t) = L_\mu w_t + f(\mu, w_t) \tag{22}$$

where $w(t) = (w_1(t), w_2(t), w_3(t))^T \in R^3$, $w_t(\theta) = w(t+\theta)$ and $L_w : C \to R^3$, $f : R \times C \to R^3$ are given, respectively, by

$$L_\mu(\phi) = (\tau^* + \mu)\left[\begin{pmatrix} c_{11} & c_{12} & c_{13} \\ c_{21} & c_{22} & c_{23} \\ 0 & 0 & c_{33} \end{pmatrix}\begin{pmatrix} w_{1t}(0) \\ w_{2t}(0) \\ w_{3t}(0) \end{pmatrix} + \begin{pmatrix} 0 & 0 & 0 \\ 0 & 0 & 0 \\ d_{31} & d_{32} & d_{33} \end{pmatrix}\begin{pmatrix} w_{1t}(-1) \\ w_{2t}(-1) \\ w_{3t}(-1) \end{pmatrix}\right] \tag{23}$$

and $F(\mu, w_t) = (\tau^* + \mu)(F_1, F_2, F_3)^T$ (24)

The nonlinear terms $F_1, F_2,$ and F_3 are given by

$$\begin{aligned}
F_1 &= b_{110}w_{1t}(0)w_{2t}(0) + b_{101}w_{1t}(0)w_{3t}(0) + b_{120}w_{1t}(0)w_{2t}^2(0) + b_{200}u_{1t}^2(0) \\
&\quad + b_{210}w_{1t}^2(0)w_{2t}(0) + b_{201}w_{1t}^2(0)w_{3t}(0) + b_{300}w_{1t}^3(0) + b_{020}e_{2t}^2(0) + b_{030}w_{2t}^3(0) + \dots \\
F_2 &= c_{110}w_{1t}(0)w_{2t}(0) + c_{101}w_{1t}(0)w_{3t}(0) + c_{120}w_{1t}(0)w_{2t}^2(0) + c_{200}u_{1t}^2(0) \\
&\quad + c_{210}w_{1t}^2(0)w_{2t}(0) + c_{201}w_{1t}^2(0)w_{3t}(0) + c_{300}w_{1t}^3(0) + c_{020}w_{2t}^2(0) + c_{030}w_{2t}^3(0) + \dots \\
F_3 &= d_{200}w_{1t}^2(-1) + d_{300}w_{1t}^3(-1) + d_{101}w_{1t}(-1)w_{3t}(-1) + d_{201}w_{1t}^2(-1)w_{3t}(-1) \\
&\quad + d_{002}w_{3t}^2(-1) + d_{003}w_{3t}^3(-1) + d_{011}w_{2t}(0)w_{3t}(-1) + d_{012}w_{2t}(0)w_{3t}^2(-1) + \dots
\end{aligned}$$

where

$$b_{110} = -\frac{r}{K} - \frac{\beta\alpha}{(\alpha + y^*)^2},\ b_{101} = -\frac{abm}{(a+x^*)^2(b+z^*)^2},\ b_{120} = \frac{\beta\alpha}{(\alpha+y^*)^3}$$
$$b_{102} = \frac{abm}{(a+x^*)^2(b+z^*)^3},\ b_{200} = -\frac{r}{K} + \frac{amz^*}{(a+x^*)^3(b+z^*)},\ b_{300} = \frac{amz^*}{(a+x^*)^3(b+z^*)}$$
$$b_{201} = \frac{abm}{(a+x^*)^3(b+z^*)^2},\ b_{020} = \frac{\beta\alpha x^*}{(\alpha+y^*)^3},\ b_{030} = -\frac{\beta\alpha x}{(\alpha+y^*)^4},$$
$$b_{002} = \frac{abmx^*}{(a+x^*)(b+z^*)^3},\ b_{003} = -\frac{abmx^*}{(a+x^*)(b+z^*)^4}$$
$$c_{110} = \frac{\beta\alpha}{(\alpha+y^*)^2},\ c_{120} = -\frac{\beta\alpha}{(\alpha+y^*)^3},\ c_{020} = -\frac{\beta\alpha x^*}{(\alpha+y)^3} + \frac{nz^{*2}}{(cz^*+y^*)^3}$$
$$c_{030} = \frac{\beta\alpha x^*}{(\alpha+y)^4} + \frac{ncz^{*2}}{(z^*+y^*)^4},\ c_{011} = \frac{ncy^*z^*}{(cz^*+y^*)^3},$$

$$c_{021} = \frac{nz^*(y - cz^*)}{(cz^* + y^*)^3},\ c_{012} = \frac{cny\,(2cz^* - y^*)}{(cz^* + y^*)^4},\ c_{002} = \frac{cny^{*2}}{(cz^* + y^*)^3},\ c_{003} = -\frac{c^2nz^{*2}}{(cz^* + y^*)^4},$$
$$d_{200} = -\frac{e_1amz^*}{(a + x^*)^3\,(b + z^*)},\ d_{300} = \frac{e_1amz^*}{(a + x^*)^4\,(b + z^*)},\ d_{101} = -\frac{e_1abm}{(a + x^*)^2\,(b + z^*)^2},$$
$$d_{201} = -\frac{e_1abm}{(a + x^*)^3\,(b + z^*)^2},\ d_{102} = -\frac{e_1abm}{(a + x^*)^2\,(b + z^*)^3},\ d_{011} = \frac{e_2ncy^*z^*}{(cz^* + y^*)^3},$$
$$d_{020} = -\frac{e_2nz^{*2}}{(cz^* + y^*)^3},\ d_{030} = \frac{e_2nz^{*2}}{(cz^* + y^*)^4},\ d_{002} = -\frac{ce_2ny^{*2}}{(cz^* + y^*)^3},\ d_{003} = \frac{c^2e_2nz^{*2}}{(cz^* + y^*)^4},$$
$$d_{021} = -\frac{e_2nz\,(y - cz^*)}{(cz^* + y^*)^4},\ d_{012} = -\frac{ce_2ny\,(2cz^* - y^*)}{(cz^* + y^*)^4}$$

The Riesz representation theorem [40] provides the existence of a 3×3 matrix $\eta(\theta, \mu), \theta \in [-1, 0]$, whose elements are a function of bounded variation functions, such that

$$L_\mu\phi = \int_{-1}^{0} d\eta(\theta, \mu)\phi(\theta),\ \text{for}\ \phi \in C = C([-1, 0], R^3). \tag{25}$$

In fact, we can choose

$$\eta(\theta, \mu) = (\tau^* + \mu)\begin{bmatrix} c_{11} & c_{12} & c_{13} \\ c_{21} & c_{22} & c_{23} \\ 0 & 0 & c_{33} \end{bmatrix}\delta(\theta) + (\tau^* + \mu)\begin{bmatrix} 0 & 0 & 0 \\ 0 & 0 & 0 \\ d_{31} & d_{32} & d_{33} \end{bmatrix}\delta(\theta + 1), \tag{26}$$

where δ is the Dirac delta function.

For $\phi \in C([-1, 0], R^3)$, we define

$$D_1(\mu)\phi = \begin{cases} \frac{d\phi(\theta)}{d\theta}, & -1 \le \theta < 0 \\ \int_{-1}^{0} d\eta(\theta, \mu)\phi(\theta), & \theta = 0 \end{cases} \tag{27}$$

$$D_2(\mu)\phi = \begin{cases} 0 & -1 \le \theta < 0, \\ f(\mu, \phi) & \theta = 0. \end{cases}$$

Then, (1) is equivalent to the following abstract differential equation:

$$\dot{w}(t) = D_1\mu w_t + D_2(\mu)w_t,\ \ \text{where}\ \ w_t(\theta) = w(t + \theta), \theta \in [-1, 0] \tag{28}$$

For $\psi \in C^1([0, 1], (R^3)^*)$, define

$$D_1^*\psi(s) = \begin{cases} -\frac{d\psi(s)}{ds} & 0 < s \le 1, \\ \int_{-1}^{0} d\eta^T(s, 0)\psi(-s) & s = 0. \end{cases} \tag{29}$$

For $\phi \in C([0, 1], R^3)$ and $\psi \in C^1([0, 1], (R^3)^*)$, define a bilinear inner product

$$< \psi, \phi >= \bar{\psi}(0)\phi(0) - \int_{-1}^{0}\int_{\zeta=0}^{\theta} \psi^T(\zeta - \theta)d\eta(\theta)\phi(\zeta)d\zeta, \tag{30}$$

where $\eta(\theta) = \eta(\theta, 0)$ and $D_1 = D_1(0)$ and D_1^* are adjoint operators.

Since $\pm i\omega_*\tau_*$ are $D_1(0)$'s eigenvalues, we may infer that they are also D_1^*'s eigenvalues. Also the vectors $q(\theta) = (1, \gamma_1, \delta_1)^T e^{i\omega_*\tau_*\theta}$ $(\theta \in [-1, 0])$ and $q^*(s) = \frac{1}{D}(1, \gamma_1^*, \delta_1^*)^T e^{i\omega_*\tau_* s}$ $(s \in [-1, 0])$ are the eigenvectors of $D_1(0)$ and D_1^* corresponding to the eigenvalues $i\omega_*\tau_*$ and $-i\omega_*\tau_*$, respectively. Then, $D_1(0)q(\theta) = i\tau_*\omega_* q(\theta)$.

Based on the definition of $D_1(0)$ in 28, 26, and 28, we have

$$\gamma_1 = \frac{c_{13}c_{21} + c_{23}\,(i\omega^* - c_{11})}{c_{12}c_{23} + c_{13}\,(i\omega^* - c_{22})},$$
$$\delta_1 = \frac{(i\omega^* - c_{11})\,(i\omega^* - c_{22}) - c_{12}c_{21}}{c_{12}c_{23} + c_{13}\,(i\omega^* - c_{22})}.$$

In a similar way, the following can determined:

$$\gamma_1^* = \frac{c_{12}d_{31}e^{i\omega^*\tau^*} - d_{32}\,(i\omega^* + c_{11})\,e^{i\omega^*\tau^*}}{c_{21}d_{32} - d_{31}\,(i\omega^* + c_{22})\,e^{i\omega^*\tau^*}},$$
$$\delta_1^* = \frac{(i\omega^* + c_{11})\,(i\omega^* + c_{22}) - c_{12}c_{21}}{c_{21}d_{32} - d_{31}\,(i\omega^* + c_{22})\,e^{i\omega^*\tau^*}}.$$

We must ascertain the value of D in order to guarantee that $< q^*(s), q(\theta) >= 1$ and $< q^*(s), \bar{q}(\theta) >= 0$. Thus, we get $< q^*(s), q(\theta) >= 1$. Hence, from $< q^*(s), q(\theta) >= 1$, we have

$$\bar{D} = 1 + \gamma_1\bar{\gamma}_1^* + \delta_1\bar{\delta}_1^* + \tau^* e^{-i\omega_*\tau_*}\bar{\delta}_1^*\,(d_{31} + d_{32}\gamma_1 + d_{33}\delta_1)\,.$$

The features of Hopf bifurcation are obtained by using the procedure given in Hassard [39], and computationally, via a method similar to Song and Wei [41], as follows

$$\begin{aligned}
g_{20} &= \frac{\tau_*}{\bar{D}}\Big[b_{200} + b_{020}\gamma_1^2 + b_{002}\delta_1^2 + b_{110}\gamma + b_{101}\delta + \bar{\gamma}_1^*\left(\delta_1^2 c_{002} + \gamma_1^2 c_{020} + c_{110}\gamma + c_{011}\gamma\delta\right)\\
&\quad + \bar{\delta}_1^*\left(d_{200}e^{-2i\omega_*\tau_*} + d_{101}\delta_1 e^{-2i\omega_*\tau_*} + d_{011}\gamma_1\delta_1 e^{-2i\omega_*\tau_*} + d_{002}\gamma_1^2 e^{-2i\omega_*\tau_*}\right)\Big],\\
g_{11} &= \frac{\tau_*}{\bar{D}}\Big[2b_{200} + \left(b_{101} + \bar{\gamma}_1^* c_{110}\right)(\gamma_1 + \bar{\gamma}_1) + b_{101}(\delta_1 + \bar{\delta}_1) + 2\gamma_1\bar{\gamma}_1\left(b_{020} + \bar{\gamma}_1^* c_{020}\right)\\
&\quad + 2\delta_1\bar{\delta}_1\left(b_{002} + \bar{\gamma}_1^* c_{002}\right) + \bar{\gamma}_1^*\left(\gamma_1\bar{\delta}_1 + \bar{\gamma}_1\delta_1\right)c_{011}\\
&\quad + \bar{\delta}_1^*\left(2d_{200} + d_{101}(\delta_1 + \bar{\delta}_1) + d_{011}(\bar{\gamma}_1\delta_1 + \gamma\bar{\delta}_1) + 2d_{002}\delta_1\bar{\delta}_1 + 2d_{020}\gamma_1\bar{\gamma}_1\right)\Big],\\
g_{02} &= \frac{\tau_*}{\bar{D}}\Big[b_{200} + (b_{020} + bar\gamma_1^* c_{020})\,\bar{\gamma}_1{}^2 + (b_{002} + bar\delta_1^* c_{002})\,\bar{\delta}_1{}^2 + (b_{110} + bar\gamma_1^* c_{110})\,\bar{\gamma}_1\\
&\quad + \left(b_{101} + \bar{\gamma}_1^*\bar{\gamma}_1 c_{011}\right)\bar{\delta}_1 + \bar{\delta}_1^* e^{2i\omega_*\tau_*}\left(d_{200} + d_{101}\bar{\delta}_1 + d_{011}\bar{\gamma}_1\bar{\delta}_1 + d_{002}\bar{\delta}_1{}^2 + d_{020}\bar{\gamma}_1{}^2\right)\Big],\\
g_{21} &= \frac{\tau_*}{\bar{D}}\Big[b_{201}\left(2\delta_1 + \bar{\delta}_1\right) + \left(b_{120} + \bar{\gamma}_1^* c_{120}\right)(\gamma_1^2 + 2\gamma_1\bar{\gamma}_1) + b_{210}\,(2\gamma_1 + \bar{\gamma}_1) + 3b_{300}\\
&\quad + \left(b_{110} + \bar{\gamma}_1^* c_{110}\right)\left(W_{11}^{(2)}(0) + \frac{1}{2}W_{20}^{(2)}(0) + \frac{1}{2}\bar{\gamma}_1 W_{20}^{(1)}(0) + \gamma_1 W_{11}^{(1)}(0)\right)\gamma_1^2\bar{\gamma}_1\\
&\quad + b_{101}\left(W_{11}^{(3)}(0) + \frac{1}{2}W_{20}^{(3)}(0) + \frac{1}{2}\bar{\delta}_1 W_{20}^{(1)}(0) + \delta_1 W_{11}^{(1)}(0)\right) + b_{200}\left(2W_{11}^{(1)}(0) + W_{20}^{(1)}(0)\right)\\
&\quad + \left(b_{020} + \bar{\gamma}_1^* c_{020}\right)\left(\bar{\gamma}_1 W_{20}^{(2)}(0) + 2\gamma_1 W_{11}^{(2)}(0)\right) + 3\left(b_{030} + \bar{\gamma}_1^* c_{030}\right) + b_{102}(\delta_1^2 + 2\delta_1\bar{\delta}_1)
\end{aligned}$$

$$
\begin{aligned}
&+\left(b_{002}+\bar{\gamma}_1^* c_{002}\right)\left(\bar{\delta}_1 W_{20}^{(3)}(0)+2\delta_1 W_{11}^{(3)}(0)\right)+3\left(b_{003}+\bar{\gamma}_1^* c_{003}\right)\delta_1^2\bar{\delta}_1\\
&+c_{011}\bar{\gamma}_1^*\left(\gamma_1 W_{11}^{(3)}(0)+\bar{\gamma}_1\frac{1}{2}W_{20}^{(3)}(0)+\frac{1}{2}\bar{\delta}_1 W_{20}^{(2)}(0)+\delta_1 W_{11}^{(2)}(0)\right)+c_{012}\bar{\gamma}_1^*(\delta_1^2\bar{\gamma}_1+2\gamma_1\delta_1\bar{\delta}_1)\\
&+c_{021}\bar{\gamma}_1^*\left(\gamma_1^2\bar{\delta}_1+\gamma_1\bar{\gamma}_1\delta_1\right)+d_{003}\bar{\delta}_1^*\left(W_{20}^{(3)}(-1)e^{i\omega_*\tau_*}\bar{\delta}_1+2W_{11}^{(3)}(-1)e^{-i\omega_*\tau_*}\delta_1\right)\\
&+3d_{300}\bar{\delta}_1^* e^{-i\omega_*\tau_*}+3d_{030}\bar{\delta}_1^*\gamma_1^2\bar{\gamma}_1 e^{-i\omega_*\tau_*}+d_{200}\bar{\delta}_1^*\left(W_{20}^{(1)}(-1)e^{i\omega_*\tau_*}+2W_{11}^{(1)}(-1)e^{-i\omega_*\tau_*}\right)\\
&+3d_{003}\bar{\delta}_1^*\delta_1^2\bar{\delta}_1 e^{-i\omega_*\tau_*}+d_{020}\bar{\delta}_1^*\left(W_{20}^{(2)}(-1)e^{i\omega_*\tau_*}\bar{\gamma}_1+2W_{11}^{(2)}(-1)e^{-i\omega_*\tau_*}\gamma_1\right)\\
&+d_{101}\bar{\delta}_1^*\left(\left(W_{11}^{(3)}(-1)+\delta_1 W_{11}^{(1)}(-1)\right)e^{-i\omega_*\tau_*}+\frac{1}{2}\left(W_{20}^{(3)}(-1)+\bar{\delta}_1 W_{20}^{(1)}(-1)\right)e^{i\omega_*\tau_*}\right)\\
&+d_{011}\bar{\delta}_1^*\left(\gamma_1 W_{11}^{(3)}(0)+\bar{\gamma}_1\frac{1}{2}W_{20}^{(3)}(0)+\frac{1}{2}\bar{\delta}_1 W_{20}^{(2)}(0)+\delta_1 W_{11}^{(2)}(0)\right)\\
&+d_{011}\bar{\delta}_1^*\left(\left(\gamma_1 W_{11}^{(3)}(-1)+\delta_1 W_{11}^{(1)}(-1)\right)e^{-i\omega_*\tau_*}+\frac{1}{2}\left(\bar{\gamma}_1 W_{20}^{(3)}(-1)+\bar{\delta}_1 W_{20}^{(1)}(-1)\right)e^{i\omega_*\tau_*}\right)\\
&+d_{012}\bar{\delta}_1^*\left(\bar{\gamma}_1\delta_1^2+2\bar{\gamma}_1\delta_1\bar{\delta}_1\right)e^{-i\omega_*\tau_*}+d_{021}\bar{\delta}_1^*\left(\bar{\delta}_1\gamma_1^2+2\bar{\delta}_1\gamma_1\bar{\gamma}_1\right)e^{-i\omega_*\tau_*}\\
&+d_{102}\bar{\delta}_1^*\left(\delta_1^2+2\delta_1\bar{\delta}_1\right)e^{-i\omega_*\tau_*}+d_{201}\bar{\delta}_1^*\left(\bar{\delta}_1+2\bar{\delta}_1\right)e^{-i\omega_*\tau_*}\Big],
\end{aligned}
$$

where
$$
\begin{aligned}
W_{20}(\theta)&=\frac{ig_{20}}{\sigma^*\tau^*}q(0)e^{i\theta\sigma^*\tau^*}+\frac{i\bar{g}_{02}}{3\sigma^*\tau^*}\bar{q}(0)e^{-i\theta\sigma^*\tau^*}+E_1 e^{2i\theta\sigma^*\tau^*},\\
W_{11}(\theta)&=-\frac{ig_{11}}{\sigma^*\tau^*}q(0)e^{i\theta\sigma^*\tau^*}+\frac{i\bar{g}_{11}}{\sigma^*\tau^*}\bar{q}(0)e^{-i\theta\sigma^*\tau^*}+E_2,
\end{aligned}
$$

and $E_1=(E_1^1,E_1^2,E_1^3)^T$, and $E_2=(E_2^1,E_2^2,E_2^3)^T$ are both constant vectors in R^3. After calculation, we get $E_1=2G_1^{-1}G_2$ and $E_2=2G_3^{-1}G_4$ with

$$
G_1=\begin{bmatrix} 2i\omega_*-c_{11} & -c_{12} & -c_{13}\\ -c_{21} & 2i\omega^*-c_{22} & -c_{23}\\ -d_{31}e^{-2i\omega_*\tau_*} & -d_{32}e^{-2i\omega_*\tau_*} & 2i\sigma^*-c_{33}-d_{33}e^{-\omega_*\tau_*}\end{bmatrix},
$$

$$
G_2=\begin{bmatrix} b_{200}+b_{020}\gamma_1^2+b_{002}\delta_1^2+b_{110}\gamma+b_{101}\delta\\ \delta_1^2 c_{002}+\gamma_1^2 c_{020}+c_{110}\gamma+c_{011}\gamma\delta\\ d_{200}e^{-2i\omega_*\tau_*}+d_{101}\delta_1 e^{-2i\omega_*\tau_*}+d_{011}\gamma_1\delta_1 e^{-2i\omega_*\tau_*}+d_{002}\gamma_1^2 e^{-2i\omega_*\tau_*}\end{bmatrix},
$$

$$
G_3=\begin{bmatrix} -c_{11} & -c_{12} & -c_{13}\\ -c_{21} & -c_{22} & -c_{23}\\ -d_{31} & -d_{32} & -c_{33}-d_{33}\end{bmatrix},
$$

$$
G_4=\begin{bmatrix} 2b_{200}+b_{101}(\gamma_1+\bar{\gamma}_1)+b_{101}(\delta_1+\bar{\delta}_1)+2\gamma_1\bar{\gamma}_1 b_{020}+2\delta_1\bar{\delta}_1 b_{002}\\ (\gamma_1+\bar{\gamma}_1)c_{110}+2\gamma_1\bar{\gamma}_1 c_{020}+\left(\gamma_1\bar{\delta}_1+\bar{\gamma}_1\delta_1\right)c_{011}\\ 2d_{200}+d_{101}(\delta_1+\bar{\delta}_1)+d_{011}(\bar{\gamma}_1\delta_1+\gamma\bar{\delta}_1)+2d_{002}\delta_1\bar{\delta}_1+2d_{020}\gamma_1\bar{\gamma}_1\end{bmatrix}.
$$

The parameters and delay may thus be used to express each g_{ij}. Thus, we calculate the subsequent values.

$$
B_1(0)=\frac{i}{2\tau^*\sigma^*}\left(g_{11}g_{20}-2|g_{11}|^2-\frac{|g_{02}|^2}{3}\right)+\frac{g_{21}}{2},
$$

$$n_1 = -\frac{\Re\{B_1(0)\}}{\Re\{\lambda'(\tau^*)\}},$$
$$n_2 = 2\Re(B_1(0)),$$
$$T_2 = -\frac{\Im\{B_1(0)\} + \eta_1 \Im(\lambda'(\tau^*))}{\tau^* \sigma^*}.$$

□

6. Numerical simulation

This section provides the dynamic behavior of the proposed model studied analytically in the previous sections. The *dde23* solver was used to solve the model numerically using MATLAB. Due to the lack of real values of all parameters of model (7), we assumed the values of the parameters are given below for numerical simulations:

$$r = 0.1, a = 0.5, b = 0.5, c = 0.5, n = 0.03m = 0.05, e_1 = 0.8, e_2 = 0.8 \quad (31)$$
$$\nu = 0.1, h = 0.01, k = 10, \alpha = 0.5$$

First, we study the system without delay, and then we observe the dynamics of the system with delay.

6.1. Simulation of the system without delay

We have checked that the gestation delay does not affect the existence of the equilibria; rather, it significantly depends on the infection rate β and also the rest of the parameters, but we focus on the infection rate due to the direction of this research. Delay τ has an impact on the stability of equilibrium points. We have discussed the facts below in detail.

In Figure 1, we have plotted the numerical solution of model (1) for lower infection rate $\beta = 0.0015$. The system is converged to the steady state $E_3(99.5, 0, 0.5)$. We have also determined that for the set of parameters mentioned above and for $\beta \in (0, 0.00165)$, $E_3(x_3, 0, z_3)$ exists and is stable (according to Theorem 2). It loses its stability for $\beta > 0.00165$ $(approx.)$, and consequently the predator-free equilibrium $E_2(x_2, y_2, 0)$ exists and is stable when $\beta < 0.09495$) (according to Theorem 1), and the endemic equilibrium $E^*(x^*, y^*, z^*)$ exists via a forward transcritical bifurcation (see Figure 2).

The interior equilibrium E^* is stable for $\beta < 0.1495$ $(approx.)$ (Figure 3). Periodic oscillation occurs for infections higher than this value. A Hopf bifurcation diagram takes β as the bifurcation parameter (Figure 4). Additionally, the maximum and minimum value of the periodic solution is plotted in the figure. From this figure, we conclude that the Hopf bifurcation occurs at $\beta = \beta^*$ (according to the Theorem 3).

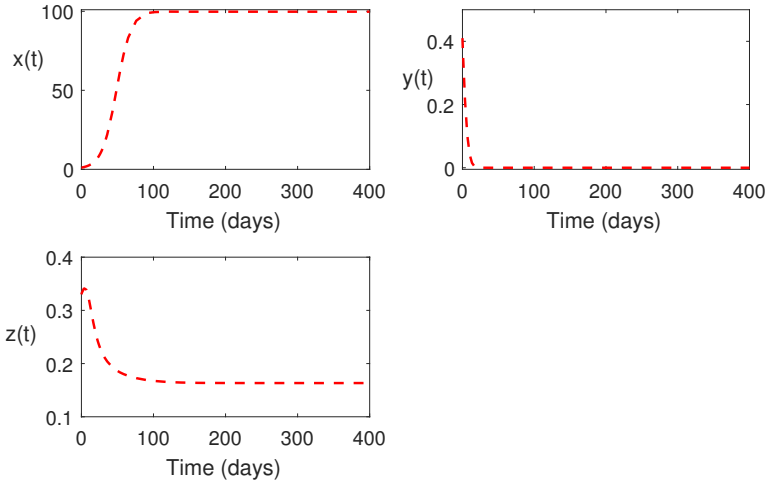

Figure 1. Numerical solution of model (1) for $\tau = 0$ is plotted for $\beta = 0.0015$. Other parameters are given in (31).

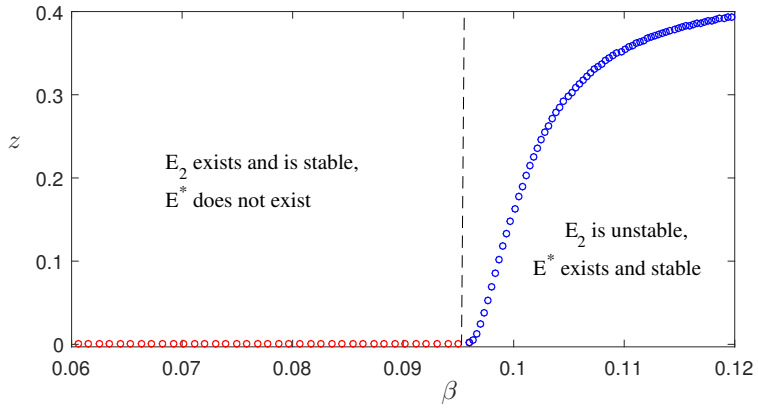

Figure 2. Steady state values of $z(t)$ plotted, taking parameters varying the infection rate β. Other parameters are given in (31).

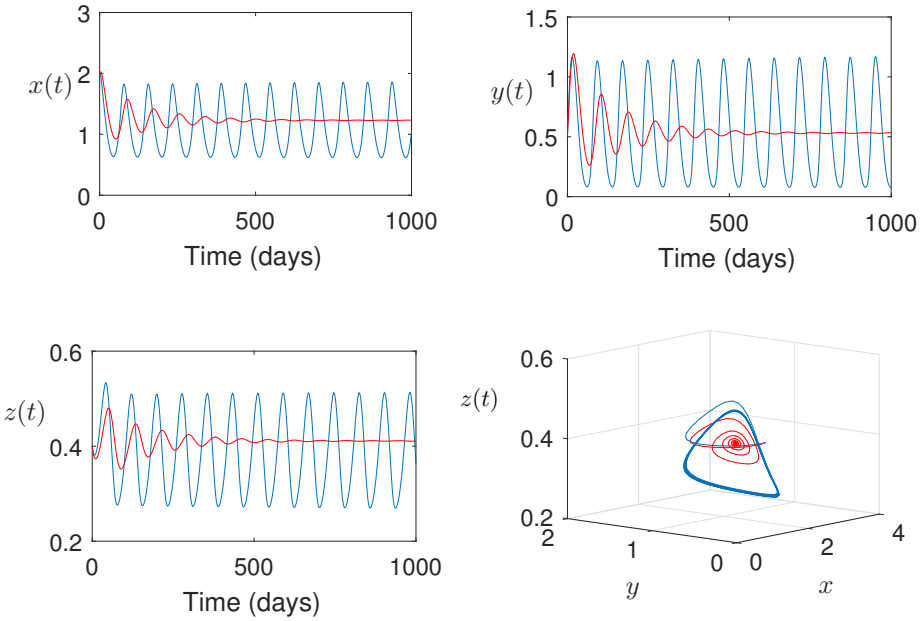

Figure 3. Numerical solutions of model (1) for $\tau = 0$ plotted for (i) $\beta = 0.152$ (red lines), and (ii) $\beta = 0.45$ (black lines). Other parameter values are the same as taken in Figure 2.

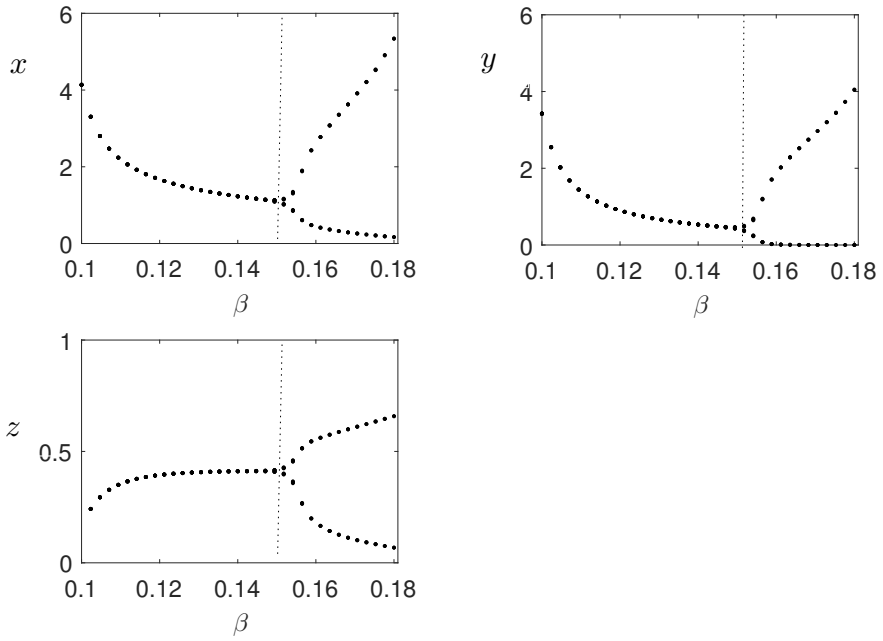

Figure 4. Hopf bifurcation taking β as the main parameter, keeping the same parameter set as in Figure 3.

6.2. Simulation of the system with delay

We have varied the delay parameter τ to study its impact on the stability of the coexisting stable state. In Figure 5, the numerical solution of the delayed system is plotted. We observed that delay causes oscillations in the solutions. Oscillations increase as the delay is enhanced.

We found from Figure 6 that the stable situation becomes unstable via a periodic solution when the delay τ crosses the threshold value $\tau^* = 4.25$ days (verifying Theorem 4). It is interesting to see that the threshold value τ^* of the delay τ depends on the values of the infection rate β. Figure 7 confirms that the coexisting equilibrium exists and is asymptotically stable for $\beta = 0.12$, and remains stable for large values of delay ($\tau = 50$).

Figure 8 shows that the initial conditions (initial population size) affect the limit cycle's stability. However, the system remains stable whenever we change the initial values of the populations. We found that $n_2 < 0$ and $T_2 > 0$, which indicates that the Hopf bifurcating periodic solutions are stable and the bifurcation is of the supercritical type (verifying Theorem 5).

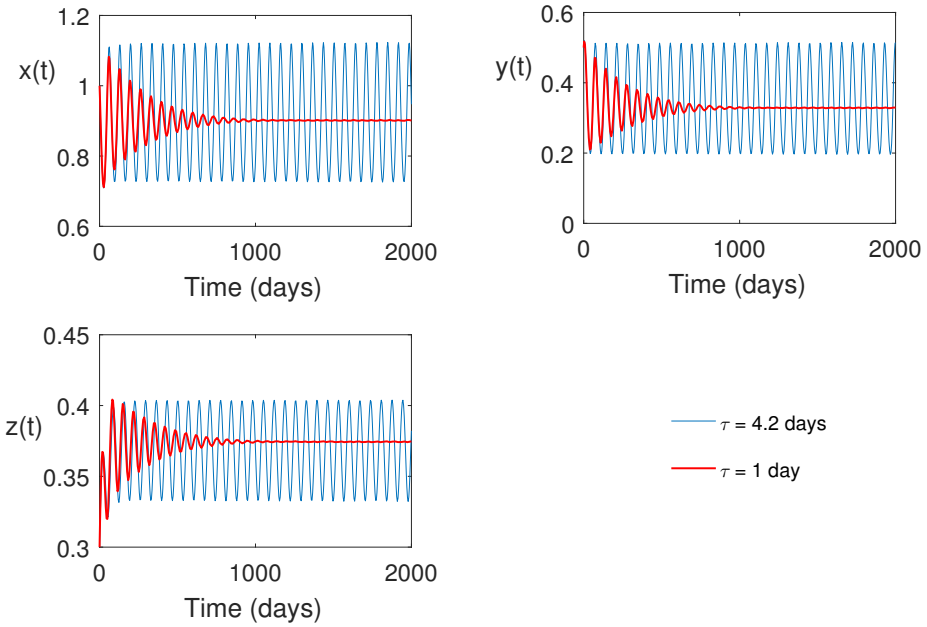

Figure 5. Numerical solutions are plotted for different values of time delay τ taking $\beta = 0.152 < \beta^*$ (i.e. system without delay is stable) and the rest of the parameters are the same as Figure 3. Here, the red lines correspond to $\tau = 1$ and the blue lines are for $\tau = 4.2$.

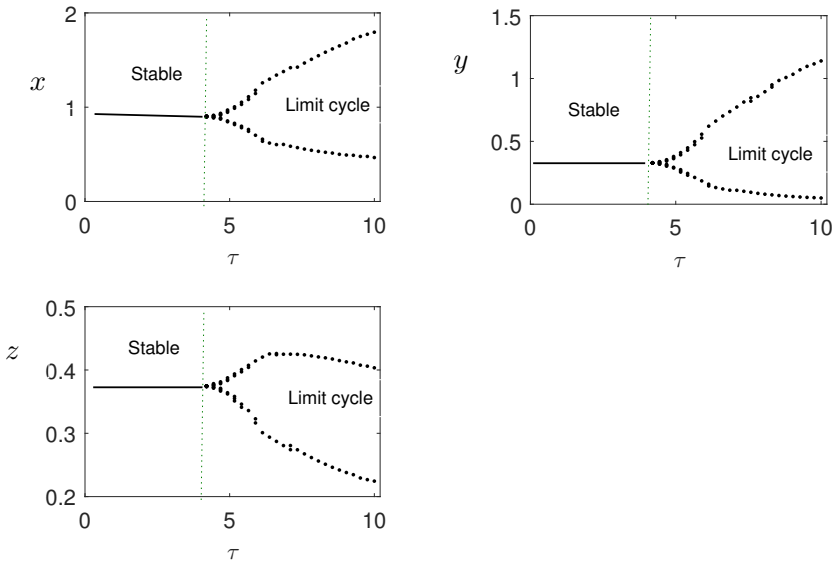

Figure 6. Hopf bifurcation taking τ as the bifurcation parameter, keeping the same parameters values as in Figure 3.

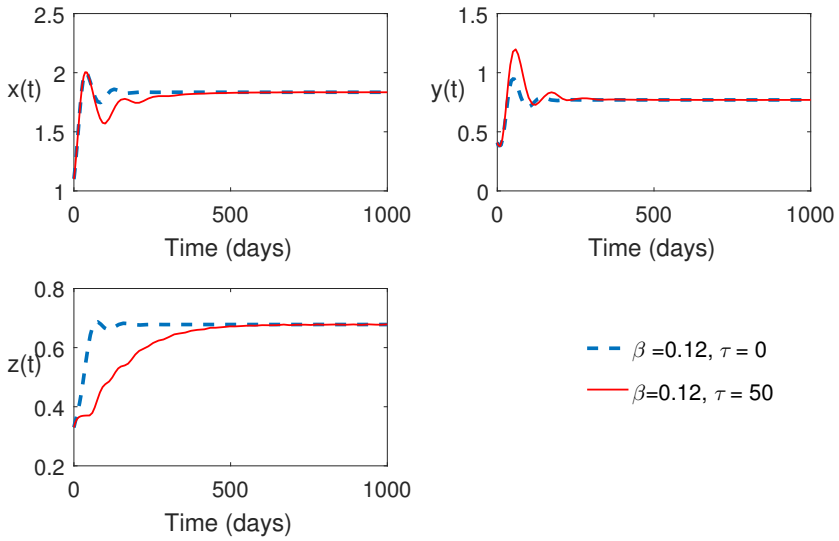

Figure 7. Numerical solutions are plotted for different values of time delay when $\beta = 0.12$. The blue lines are used for $\tau = 0$ and the red lines are used for $\tau = 50$.

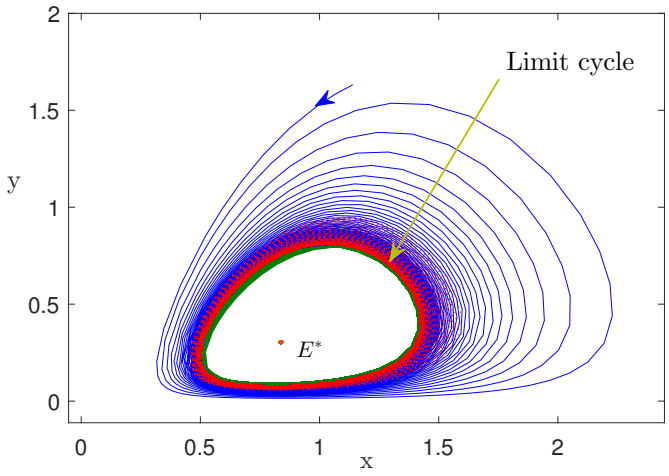

Figure 8. Phase portraits plotted in the $(x - y)$ plane with different initial conditions for $\tau = 4.2$ with the parameters values as in Figure 5.

7. Discussion and Conclusions

Eco-epidemic models with delay are mathematical frameworks used to study the interactions between ecological and epidemiological processes. These models incorporate incubation or gestation delays to account for the non-instantaneous effects of various biological interactions. Analysis of the models includes the determination of the equilibrium points and analysis of their stability using characteristic equations derived from the linearization of the delay models around the equilibrium points. Numerical simulations of these models include complex dynamics such as periodic oscillations or chaos.

In this paper, we have derived a predator-prey model including a time delay due to the gestation period of the predator. We have also considered an infection in the prey population modeled using a nonlinear term. Thus, the total prey population is divided into two sub-populations, namely the susceptible prey and the infected prey. Consumption of susceptible prey by predators is modeled using a Crowley-Martin type functional response, and consumption of infected prey using a Beddington-DeAngelis (ratio-dependent) type density dependent functional response. We have discussed the existence of all possible equilibrium points of the proposed model, and the local stability analysis around these equilibrium points has been studied for two cases: with delay and without delay. Hopf bifurcation analysis for both delay and non-delay model is also provided analytically and numerically.

From the existence analysis of equilibria, we have found that the proposed model has three equilibrium points, namely the infection-free, predator-free, and interior equilibrium points. We have provided the existence criteria of the equilibrium points. Via stability analysis, we have provided stability criteria of all the equilibria for two cases: with delay and without delay. Hopf bifurcation of the interior equilibrium point is presented for both cases.

Numerical results confirm that the proposed predator-prey model (1) has a stable disease-free equilibrium $E_2(x, 0, z)$ for infection rate belonging to a lower range ($\beta \in (0.01495, 0.1452)$). From the local stability analysis, it is found that the disease-free equilibrium point E_3 exists when the infection rate is greater than a threshold value. From the numerical stability analysis, we found that the interior

equilibrium is asymptotically stable when the conditions of Theorem 3 are satisfied. Then, Hopf bifurcation diagrams are plotted for both delay and non-delay cases. When the infection crosses the value $\beta^* = 1.525$, Hopf bifurcation occurs. Again, when the delay $\tau > \tau^* = 4.252$, Hopf bifurcation occurs via periodic oscillations (Figure 4 and 6). At a lower infection rate, the stable system remains stable, though the gestation delay is large ($\tau = 50$ days) (Figure 7).

In a nutshell, the proposed eco-epidemic model with Crowley-Martin type functional response for susceptible prey and Beddington-DeAngelis (ratio dependent) type response for infected prey is functional and can be applied to real-world phenomena.

Author contributions

H.M., S.S. Conceptualization; H.M., F.A.B.: Methodology; A.A.R., F.A.B.: Software; A.A.R., F.A.B.: Validation; H.M., F.A.B.: Formal analysis; H.M., S.S., F.A.B.: Investigation; H.M., S.S., F.A.B.: Writing-original draft preparation; S.S., F.A.B.: Writing-review and editing; S.S., F.A.B.: Supervision; A.A.R.: Project administration. All authors have read and agreed to the published version of the manuscript.

Conflict of interest

The authors declare no conflict of interest.

Acknowledgments

The authors extend their appreciation to the Deanship of Research and Graduate Studies at King Khalid University, Kingdom of Saudi Arabia - Abha, for funding this work through Large Research Project under grant number RGP2/174/45.

References

1. C. Jeffries, *Mathematical modeling in ecology: a workbook for students*, Springer Science & Business Media, (2012).
2. P. Chesson, Predator-prey theory and variability, *Annual Rev. Ecol. Syst.*, **9** (1978), 323–347.
3. M. S. Boyce, Modeling predator–prey dynamics, In: *Research techniques in animal ecology*, Columbia University Press, New York, USA, (2000), 253–87.
4. A. J. Lotka, Elements of physical biology, *Nature*, **116** (1925). https://doi.org/10.1038/116461b0
5. Volterra, V. Variations and fluctuations of a number of individuals in animal species living together, *ICES J. Marine Sci.*, **3** (1928), 3–51. https://doi.org/10.1093/icesjms/3.1.3
6. R. M. May, R. M.Anderson, Population biology of infectious diseases: part II, *Nature*, **280** (1979), 455–461. https://doi.org/10.1038/280455a0
7. Y. Xiao, L. Chen, Modeling and analysis of a predator-prey model with disease in the prey, *Math. Biosci.*, **171** (2001), 59–82. https://doi.org/10.1016/S0025-5564(01)00049-9

8. G. P. Hu, X. L. Li, Stability and Hopf bifurcation for a delayed predator–prey model with disease in the prey, *Chaos Soli. Fract.*, **45** (2012), 229–237. https://doi.org/10.1016/j.chaos.2011.11.011
9. X. Zhou, J. Cui, X. Shi, X. Song, A modified Leslie-Gower predator-prey model with prey infection, *J. Appl. Math. Comput.*, **33** (2010), 471–487. https://doi.org/10.1007/s12190-009-0298-6
10. X. Zhou, X. Shi, X. Song, The dynamics of an eco-epidemiological model with distributed delay, *Nonl. Anal. Hybrid Sys.*, **3** (2009), 685–699. https://doi.org/10.1016/j.nahs.2009.06.005
11. Z. Zhang, H. Yang, Hopf bifurcation control in a delayed predator-prey system with prey infection and modified Leslie-Gower scheme, *Abst. Appl. Anal.*, **2013** (2013), 1–11. https://doi.org/10.1155/2013/704320
12. M. Haque, S. Sarwardi, S. Preston, E. Venturino, Effect of delay in a Lotka–Volterra type predator–prey model with a transmissible disease in the predator species, *Math. Biosci.*, **234** (2011), 47–57. https://doi.org/10.1016/j.mbs.2011.06.009
13. E. Venturino, Epidemics in predator-prey models: disease in the predators, *IMA J. Math. Appl. Med. Biol.*, **19** (2002), 185–205. https://doi.org/10.1093/imammb/19.3.185
14. Y. P. Zhang, M. J. Ma, P. Zuo, X. Liang, Analysis of a eco-epidemiological model with disease in the predator, *Appl. Mech. Material.*, **536** (2014), 861–864. https://doi.org/10.4028/www.scientific.net/AMM.536-537.861
15. Y. P. Zhang, M. J. Ma, P. Zuo, X. Liang, Analysis of a eco-epidemiological model with disease in the predator, *Appl. Mech. Material.*, **536** (2014), 861–864.
16. Q. Dong, W. Ma, W. M. Sun, The asymptotic behavior of a Chemostat model with Crowley–Martin type functional response and time delays, *J. Math. Chem.*, **51** (2013), 1231–1248. https://doi.org/10.1007/s10910-012-0138-z
17. A. P. Maiti, B. Dubey, Stability and bifurcation of a fishery model with Crowley-Martin functional response, *Int. J. Bifur. Chaos.*, **27** (2017), 1750174.
18. J. P. Tripathi, S. Tyagi, S. Abbas, Global analysis of a delayed density dependent predator-prey model with Crowley-Martin functional response, *Commun. Nonl. Sci. Numer. Simul.*, **30** (2016), 45–69. https://doi.org/10.1016/j.cnsns.2015.06.008
19. F. Wei, Q. Fu, Hopf bifurcation and stability for predator-prey system with Beddington-DeAngelis type functional response and stage structure for prey incorpting refuge, *Appl. Math. Model.*, **40** (2016), 126–134. https://doi.org/10.1016/j.apm.2015.04.042
20. S. Sarwardi, M. Haque, S. Hossain, Analysis of Bogdanov–takens bifurcations in a spatiotemporal harvested-predator and prey system with Beddington–DeAngelis-type response function, *Nonlinear Dyn.*, **100** (2020), 1755–1778. https://doi.org/10.1007/s11071-020-05549-y
21. M. S. Rahman, M. S. Islam, S. Sarwardi, Effects of prey refuge with Holling type IV functional response dependent prey predator model, *Int. J. Model. Simul.*, (2023), 1–19. https://doi.org/10.1080/02286203.2023.2178066
22. S. Sarwardi, M. Haque, E. Venturino, Global stability and persistence in LG–Holling type II diseased predator ecosystems, *J. Biol. Phys.*, **37** (2011), 91–106. https://doi.org/10.1007/s10867-010-9201-9

23. J. Huang, Y. Gong, J. Chen, Multiple bifurcations in a predator-prey system of Holling and Leslie type with constant-yield prey harvesting, *Int. J. Bifurc. Chaos.*, **23** (2013), 50164. https://doi.org/10.1142/S0218127413501642

24. N. Bairagi, D. Jana, On the stability and Hopf bifurcation of a delay-induced predator-prey system with habitat complexity, *Appl. Math. Model.*, **35** (2011), 3255–3267. https://doi.org/10.1016/j.apm.2011.01.025

25. G. Liu, J. Yan, Existence of positive periodic solutions for neutral delay Gause-type predator–prey system, *Appl. Math. Model.*, **35** (2011), 5741–5750. https://doi.org/10.1016/j.apm.2011.05.006

26. Z. Du, Y. Lv, Permanence and almost periodic solution of a model with mutual interference and time delays, *Appl. Math. Model.*, **37** (2013), 1054–1068. https://doi.org/10.1016/j.apm.2012.03.022

27. L. Deng, X. Wang, M. Peng, Hopf bifurcation analysis for a ratio-dependent predator-prey system with two delays and stage structure for the predator, *Appl. Math. Comput.*, **231** (2014), 214–230. http://dx.doi.org/10.1016/j.amc.2014.01.025

28. P. Sen, S. Samanta, M. Y. Khan, S. Mandal, P. K. Tiwari, A seasonally forced eco-epidemic model with disease in predator and incubation delay, *J. Biol. Syst.*, **31** (2023), 921–962. https://doi.org/10.1142/S0218339023500328

29. A. A. Shaikh, H. Das, N. Ali, Study of LG-Holling type III predator–prey model with disease in predator, *J. Appl. Math. Comput.*, **58** (2017), 235–255. https://doi.org/10.1007/s12190-017-1142-z

30. L. Wang, R. Xu, G. Feng, Modelling and analysis of an eco-epidemiological model with time delay and stage structure, *J. Appl. Math. Comput.*, **50** (2015), 175–197. https://doi.org/10.1007/s12190-014-0865-3

31. S. Kant, V. Kumar, Stability analysis of predator–prey system with migrating prey and disease infection in both species, *Appl. Math. Model.*, **42** (2016), 509–539. https://doi.org/10.1016/j.apm.2016.10.003

32. F. A. Basir, M. H. Noor, A model for pest control using integrated approach: impact of latent and gestation delays, *Nonlinear Dyn.*, **108** (2022), 1805–1820. https://doi.org/10.1007/s11071-022-07251-7

33. S. G. Mortoja, P. Panja, S. K. Mondal, Dynamics of a predator-prey model with nonlinear incidence rate, Crowley-Martin type functional response and disease in prey population, *Ecol. Gen. Genom.*, **10** (2019), 100035. https://doi.org/10.1016/j.egg.2018.100035

34. L. Zha, J. A. Cui, X. Zhou, Ratio-dependent predator–prey model with stage structure and time delay, *Int. J. Biomath.*, **5** (2012), 1250014. https://doi.org/10.1142/S1793524511001556

35. R. Xu, Z. Ma, Stability and Hopf bifurcation in a ratio-dependent predator–prey system with stage structure, *Chaos Soli. Fract.*, **38** (2008), 669–684. https://doi.org/10.1016/j.chaos.2007.01.019

36. F. A. Basir, Y. Takeuchi, S. Ray, Dynamics of a delayed plant disease model with Beddington-DeAngelis disease transmission, *Math. Biosci. Eng.*, **18** (2021), 583–599. https://doi.org/10.3934/mbe.2021032

37. R. J. Bauer, G. Mo, W. Krzyzanski, Solving delay differential equations in S-ADAPT by method of steps, *Comput. Methods Programs Biomed.*, **111** (2013), 715–734. https://doi.org/10.1016/j.cmpb.2013.05.026

38. G. Birkhoff, G. C. Rota, *Ordinary Differential Equations*, Ginn Boston, (1982).

39. B. D. Hassard, N. D. Kazarinoff, Y. H. Wan, *Theory and applications of Hopf bifurcation*, Cambridge University Press Cambridge, (1981).

40. J. K. Hale, S. M. Verduyn, *Introduction to Functional Differential Equations*, Springer-Verlag, (1993).

41. Y. Song, J. Wei, Bifurcation analysis for Chen's system with delayed feedback and its application to control of chaos, *Chaos Soli. Fract.*, **22** (2004), 75–91. https://doi.org/10.1016/j.chaos.2003.12.075

AIMS Press